Single molecule sensing with carbon nanotube devices

Yongki Choi,[1] Patrick C. Sims,[1] Tivoli J. Olsen,[2] Mariam Iftikhar,[2] Brad L. Corso,[1] O. Tolga Gul,[1] Gregory A. Weiss,[2] and Philip G. Collins[1*]

[1]Dept. of Physics and Astronomy and [2]Dept. of Chemistry, University of California at Irvine, Irvine CA USA 92697

ABSTRACT

Nanoscale electronic devices like field-effect transistors have long promised to provide sensitive, label-free detection of biomolecules. In particular, single-walled carbon nanotubes have the requisite sensitivity to detect single molecule events and sufficient bandwidth to directly monitor single molecule dynamics in real time. Recent measurements have demonstrated this premise by monitoring the dynamic, single-molecule processivity of three different enzymes: lysozyme, protein Kinase A, and the Klenow fragment of DNA polymerase I. In each case, recordings resolved detailed trajectories of tens of thousands of individual chemical events and provided excellent statistics for single-molecule events. This electronic technique has a temporal resolution approaching 1 microsecond, which provides a new window for observing brief, intermediate transition states. In addition, the devices are indefinitely stable, so that the same molecule can be observed for minutes and hours. The extended recordings provide new insights into rare events like transitions to chemically-inactive conformations.

Keywords: single molecule, carbon nanotube, biosensor, enzymology, lysozyme, protein kinase, DNA polymerase

1. INTRODUCTION

Conceptually, it is easy to imagine shrinking bioelectronic interfaces down to the scale of single molecules, so that biochemistry could be monitored at the molecular level. The challenges of achieving such devices are purely technological. Single molecule bioelectronic devices would require feature sizes smaller than state-of-the-art semiconductor electronics, and devices would have unique requirements for sensitivity and stability.

Despite these challenges, the successful fabrication of devices at the single molecule scale would have enormous rewards. Single molecule bioelectronics could provide a breakthrough technology for monitoring the activity and behavior of molecules. This activity includes stochastic fluctuations, instantaneous dynamics, and nonequilibrium behaviors, all of which are key to a molecule's functionality but averaged out in conventional, ensemble characterization. Single molecule measurements could provide unique insights into the unusual kinetics of a genetically mutated protein or the effectiveness of a pharmacological inhibitor, grand challenges for biology and biophysics in the coming century. The potential benefits of observing chemistry with single molecule resolution has led to the invention and development of various single-molecule techniques. Single molecule fluorescence, specifically Förster resonance energy transfer (FRET), has become a standard tool for single molecule biochemistry.[1]

Recently, we have developed a new single molecule technique that exceeds the resolution of FRET by using an electronic, rather than optical, mechanism. Using carbon nanotube field effect transistors,[2] we have developed a type of electronic device that directly reports molecular binding events as an electronic signal. Here, we describe single molecule recordings using three different enzymes: lysozyme,[2-4] cAMP-dependent protein kinase (PKA),[5] and the Klenow fragment of DNA polymerase I (KF).[6] In all three cases, the nanocircuit technique continuously recorded the dynamic motions of a single biomolecule. The kinetics of complex, biochemical reactions were observed in real-time through many thousands of binding events with molecule-by-molecule precision. Our reports on these studies include the observation of memory effects, dynamic disorder, and processive variability, all of which are hidden in conventional, ensemble measurements.[2-6] In addition, successful experiments with three different enzymes prove the versatility of this electronic approach and suggest new avenues for conducting single molecule research.

2. DEVICE FABRICATION

Fabrication of single molecule sensors involved two main aspects. First, electronic devices must be made sufficiently sensitive to transduce single molecule events. Second, those devices must be biofunctionalized for a particular use or

target. Our work selected single-walled carbon nanotubes (SWNTs) as the best-suited nanoelectronic conductors. SWNTs are hollow graphitic cylinders that conduct electricity along their outer, exposed surfaces. As high mobility, quasi-one-dimensional conductors, these wires are excellent candidates for sensing applications.[7-11] The charge carriers in a pristine, isolated SWNT scatter infrequently, so the resistance of a SWNT can be a sensitive indicator of additional scattering caused by environmental surface interactions.[12] Furthermore, the one-dimensionality of SWNTs means that carriers cannot simply redistribute away from such a scattering site, as they do in metal films or even atomically-thin graphene. In a one-dimensional wire, every individual electron that contributes to the electrical current will directly interact with a single scattering site.

To make the best use of these properties, SWNT devices were fabricated in the dilute limit of individual, isolated SWNTs. The SWNTs were synthesized by chemical vapor deposition on 4" silicon wafers, and then electrically contacted by optical lithography. While the synthesis was controlled to produce dilute, well-separated SWNTs, wafer-scale lithography allowed thousands of devices to be fabricated in parallel. Individual devices were electrically characterized and categorized and imaged by atomic force microscopy. In addition, devices were coated with a layer of polymer or oxide to minimize electronic fluctuations and protect the metal electrodes from electrolyte solutions. This protective layer was selectively removed, using electron beam or optical lithography, to expose short segments of the SWNT conductor. The length of exposed SWNTs was typically 0.5 to 1.5 μm and could be varied on a device-by-device basis depending on the protein being investigated.

For the biofunctionalization of SWNTs, covalent and noncovalent techniques are possible. While we have had success with both techniques at the single molecule scale, noncovalent techniques have resulted in better signal-to-noise ratios because they introduce the least disruption to the SWNT's electronic band structure and its chemical stability. Consequently, we restrict our focus here to the noncovalent method, which is outlined schematically in Fig. 1. In this method, pyrene-maleimide molecules serve as linkers between the molecule of interest and the SWNT sidewalls.[13] The pyrene end of these linkers adheres to the SWNT sidewall through strong π-π interactions,[14, 15] while the maleimide end can form stable thioether bonds with free surface cysteine groups of proteins (Fig. 1a).[13]

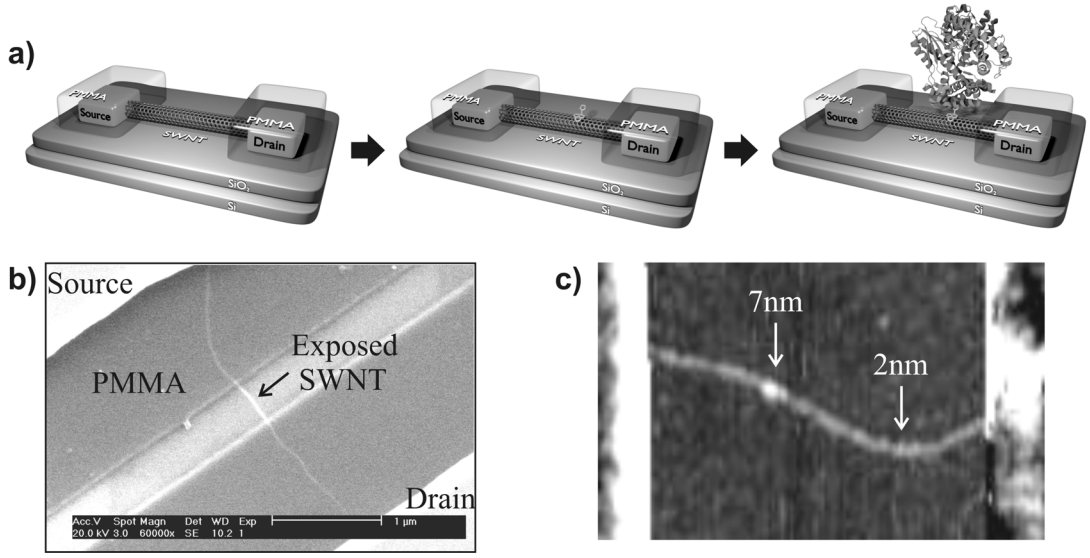

Figure 1. Single molecule carbon nanotube devices. (a) A pristine SWNT-FET is first fabricated with a passivating oxide or polymer so that only a short portion of SWNT is exposed to the environment. Next, the device is dilutely coated with pyrene-maleimide linker molecules, which then allows straightforward bioconjugation. (b) SEM image of a pristine SWNT-FET, showing the use of PMMA as a passivation layer. (c) In-liquid AFM image of a device after bioconjugation. Arrows indicate a single molecule attachment and the SWNT.

Restricting biofunctionalization to just one molecular attachment was accomplished by varying the concentrations of linker molecules and protein. Typically, devices were soaked in a 1 mM solution of pyrene-maleimide (in ethanol) and then rigorously rinsed multiple times to leave only a few linkers on each SWNT. Next, devices were incubated in a buffered solution of protein. We synthesized and purified custom protein variants by mutagenesis to contain only one surface cysteine. These cysteine groups provided a specific attachment site so that each protein attachment occurred

with the same orientation. After incubation, protein attachments were counted by atomic force microscopy. We empirically determined the attachment probability and then adjusted the incubation concentration (10 – 100 mg/ml) and time appropriately (30 – 90 min).

Once an attachment protocol had been developed for a particular protein, the yield of devices that produce single-molecule electronic signals was between 50 and 80%. Fig. 1c shows an in-liquid AFM image of a typical device after bioconjugation. With care and proper rinsing, the device surfaces remained clean enough to clearly image the SWNT and the attached biomolecules (arrows). Note that the typical SWNT diameter is much smaller than most proteins, helping to make protein identification in AFM images straightforward.

3. LYSOZYME

Lysozyme is an innate immune-system enzyme that attacks bacterial cell walls to cause cell lysis. Specifically, the enzyme catalyzes the hydrolysis of glycosidic bonds that make up the peptidoglycan layer of a bacterial cell wall. X-ray crystal structures reveal that lysozyme has two domains, and that the enzyme opens and closes around a hinge domain when binding and unbinding peptidoglycan.[16, 17] Single-molecule FRET studies have observed this hinge bending motion during binding and unbinding.[18] However, careful observations also determined that successful catalysis does not always accompany mechanical hinge motion. When the hinge opens and closes at rates of 10 – 80 s^{-1}, glycosidic bonds are being broken. Faster motions in a distinct range of 200 – 400 s^{-1} do not result in hydrolysis, even when peptidoglycan appears to be properly bound.[18-21]

We synthesized a single-cysteine, pseudo-wild-type variant of the lysozyme from T4 bacteriophage (with the following mutations: C54T / C97A / S90C, hereafter referred to generically as "lysozyme"), and then these molecules to SWNT devices using the protocol described above. Devices were then measured in phosphate buffered saline (PBS; 138 mM NaCl, 2.7 mM KCl, 8.1 mM Na_2HPO_4, 1.5 mM KH_2PO_4, pH 7.5) with and without peptidoglycan substrates.[2-4] Uninterrupted recording of the source-drain current $\Delta I(t)$ at constant bias was typically conducted for 600 s.

Fig. 2 summarizes electronic data collected from a single lysozyme device. In general, we focus on current fluctuations $\Delta I(t)$ away from an average baseline. As shown in Fig. 2a, the fluctuations vary widely over long durations. At higher resolution, the recordings can be easily split into three categories of activity, as illustrated by Fig. 2b. Approximately 5% of the recording exhibits a quiet $\Delta I(t)$ with insignificant fluctuations. The remaining 95% of recordings showed two-level oscillations with either slow or fast rates that matched previous FRET measurements. Unlike FRET, however, the measurements in Fig. 2a directly resolved a single molecule changing back and forth between its slow and fast types of motion. Both slow and fast excursions completely disappeared when peptidoglycan substrate was removed from the measurement solution.

To quantitatively evaluate the current fluctuations $\Delta I(t)$, histograms were built of the low (τ_{lo}) and high (τ_{hi}) durations spent during each individual $\Delta I(t)$ excursion. All of the fast-rate portions of a 600-s data set were combined together into one data subset, and the slow-rate portions were treated as a separate subset. Fig. 2c shows representative τ_{hi} and τ_{lo} distributions corresponding to the slow and the fast types of motion depicted in Fig. 2b. All four distributions fit single mean time constants $<\tau_{lo}>$ or $<\tau_{hi}>$, with an average turnover rate k_{cat} calculated as $k_{cat} = (<\tau_{lo}> + <\tau_{hi}>)^{-1}$.[19] During the slower, catalytically effective motions, k_{cat} = 15.4 s^{-1} for this particular molecule. During the faster, catalytically nonproductive motions, k_{cat} = 316 s^{-1}. Approximately 50% of the time, $I(t)$ oscillated slowly at a rate of 15 to 60 s^{-1}. During the remaining time, $I(t)$ oscillated with the same magnitude but at much rapidly at rates of 200 to 400 s^{-1}. Single molecule FRET measurements have observed similar two rates, with lysozyme molecules in either the faster, nonproductive state or the slower, catalytically productive one.[18, 20-22]

To investigate the effect of the cross-links of the native peptidoglycan substrate on lysozyme's activity, we synthesized a linear peptidoglycan substrate that lacked the peptide cross-links. Next, single molecule lysozyme devices were probed with the cross-linked and linear types of substrate. Fig. 3 depicts the difference in activity observed for the two types of substrate, using three gray scales to visually identify the slow, fast, and inactive portions of the data. Long duration (> 600 s) of the SWNT measurements allowed direct observation of interconversion from one type of behavior to another. Pie charts in Fig. 4 summarize the average behaviors observed in one 600 s data set. When processing the linear peptidoglycan substrates, the periods of fast, nonproductive motions are much shorter and less frequent, and the total time spent in such motions decreased from 43% to only 7% of the total record. Average rates shown in the pie chart indicate that removal of cross-links was also accompanied by 15 to 20% increases in k_{cat} for both the fast- and slow-rate states. In the absence of cross-links, lysozyme continuously catalyzes the hydrolysis of many hundreds of glycosidic

bonds over 10 to 30 seconds without any interruption, indicating a processive enzyme.[20] Furthermore, the role of the fast, nonproductive activity was associated with the lysozyme encountering cross-links where lysozyme transits from one strand to another, bypassing a cross-link.

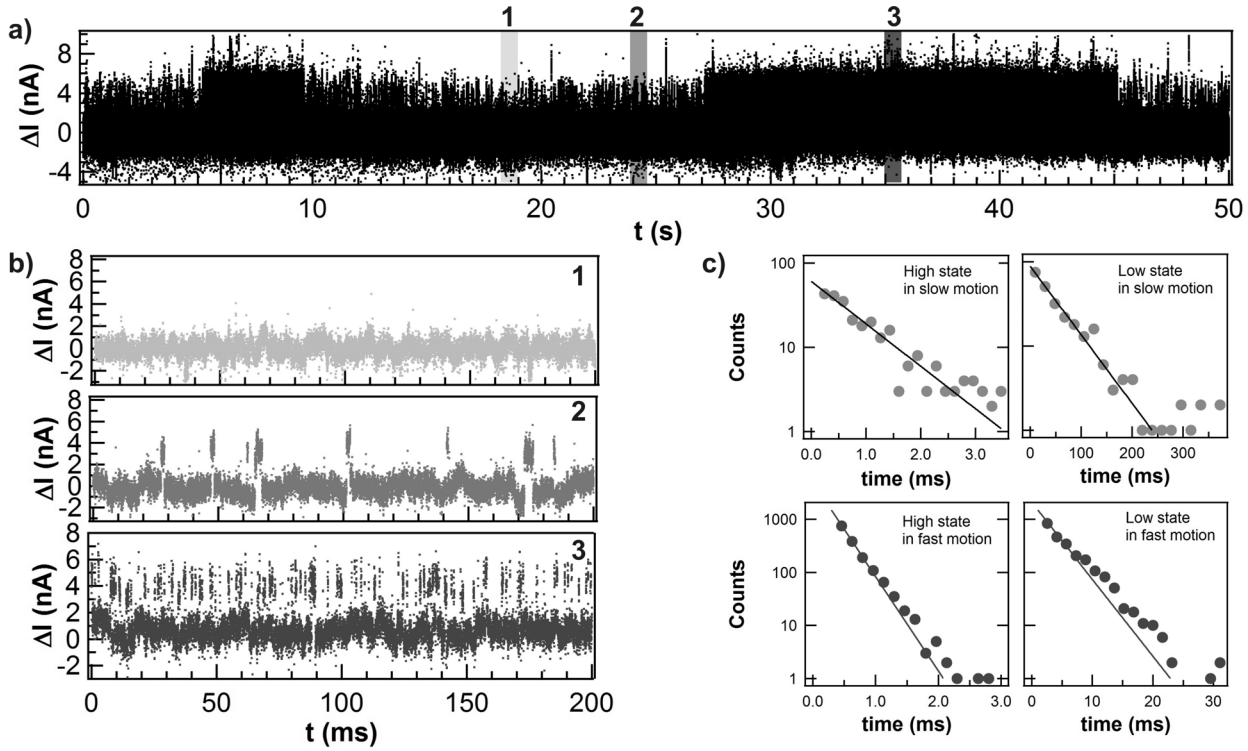

Figure 2. Electronic recordings of lysozyme activity. (a) Fluctuations of current (at a constant source-drain bias of 100 mV) encode the activity of the attached molecule. (b) Three distinct types of activity shown in high resolution. (c) Single-molecule probability distributions for the timing of transitions.

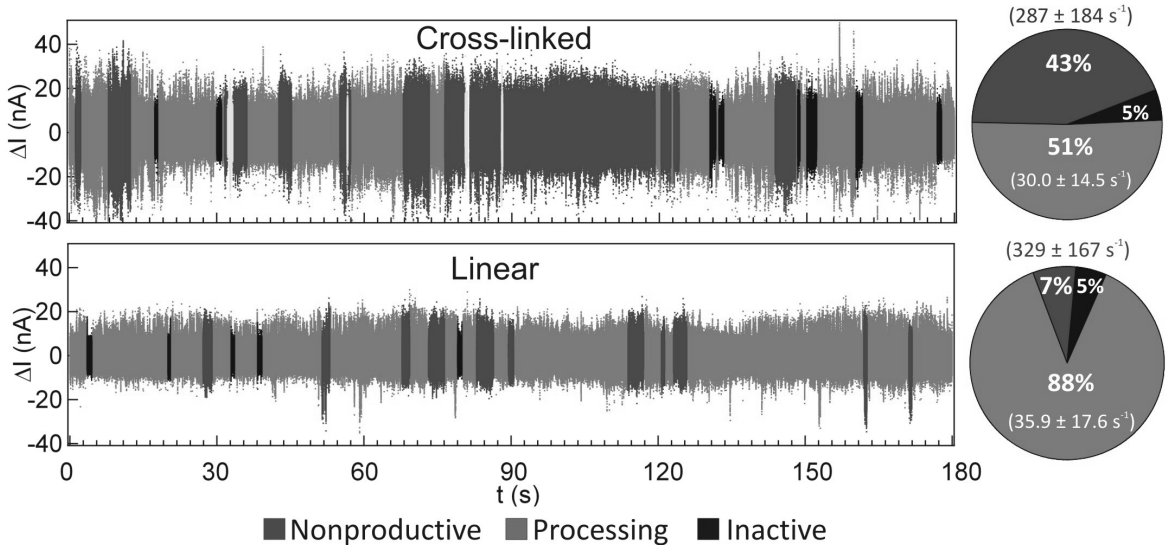

Figure 3. Comparative recordings of lysozyme activity in the presence of natural, cross-linked peptidoglycan substrate and a synthetic, linear version without cross-links. Charts at right summarize the dramatic decrease in fast, nonproductive motions.

4. DNA POLYMERASE I

In all living organisms, DNA polymerases replicate and repair DNA. Among the many families of DNA polymerases, all share a common catalytic subdomain that is responsible for the actual DNA replication. The subdomain operates by recognizing and then incorporating a complementary deoxyribonecleodtide triphosphate (dNTP) into a DNA template strand.[23, 24]

The Klenow fragment of DNA polymerase I (KF) is one example enzyme that has been widely studied due to its simplicity in activity and expression. As with lysozyme, we synthesized a single-cysteine KF variant (D355A / E357A / L790C / C907S, hereafter referred to as KF), and then attached it to SWNT devices.[6] The KF variant had no proofreading activity, as its exonuclease domain was deactivated by the mutations. Electronic measurements were performed with devices submerged in a standard buffered solution (10 mM Tris, 50 mM NaCl, 10 mM $MgCl_2$, 10 mM DTT, pH 7.8) with homopolymeric DNA template (100 nM) and an excess of either complementary or non-complementary dNTPs (10 μM). The DNA templates consisted of a M13 forward primers to which KF initially binds, annealed to a 42-base homopolymer poly(dA)$_{42}$, poly(dT)$_{42}$, poly(dC)$_{42}$, or poly(dG)$_{42}$.

Fig. 4a presents typical recordings of $\Delta I(t)$ from a single-molecule KF device probed with only poly(dA)$_{42}$ template but without dNTPs, providing the baseline noise level of the device. Fig. 4b shows that $\Delta I(t)$ excursions appeared when complementary dTTPs were introduced, whereas Fig. 4c depicts the same template mixed with noncomplementary dCTP. Measurements on the same device were separated by extensive rinsing with buffer to eliminate spurious signals caused by cross contamination. For all 16 different combinations of DNA template and dNTPs, dynamic $\Delta I(t)$ excursions were only observed when complementary dNTPs were present in the measurement buffer.

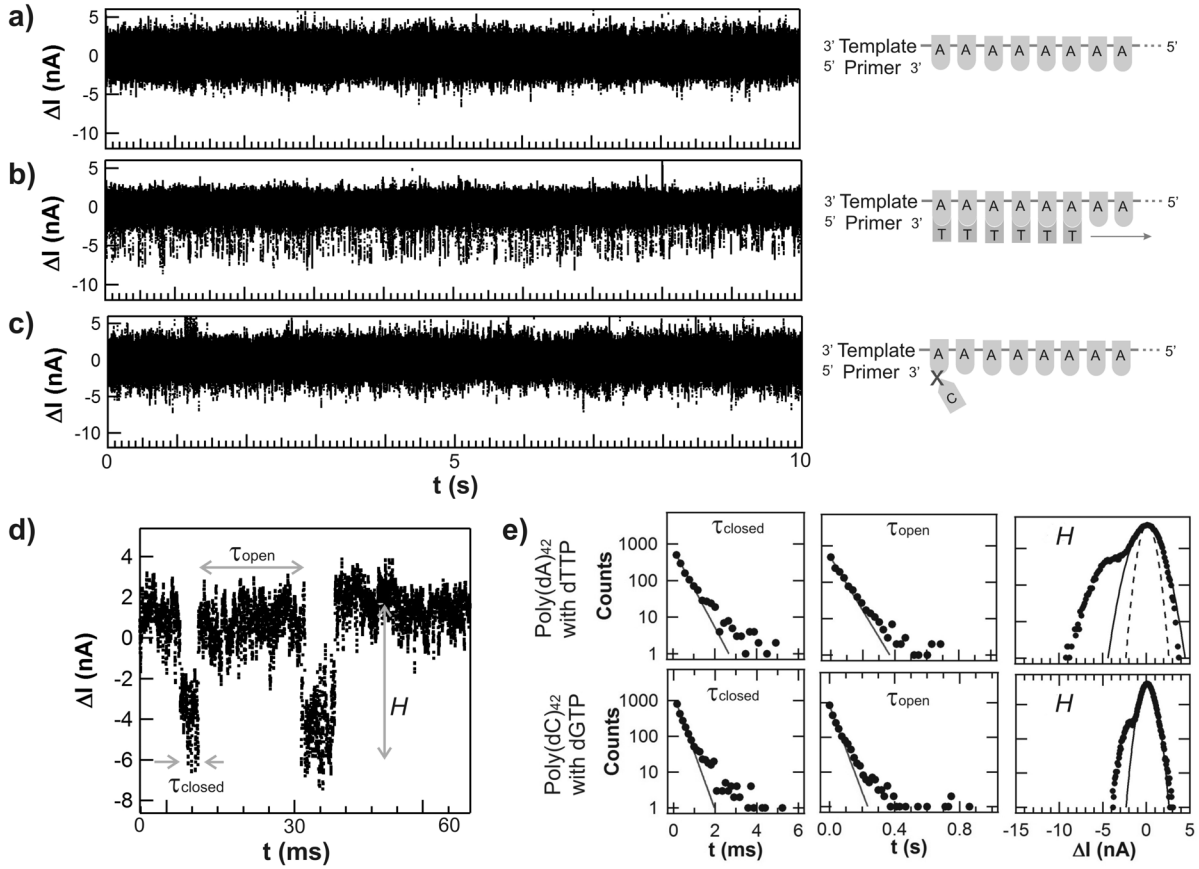

Figure 4. Electronic recordings of KF activity. (a) In the presence of primer template, single-molecule KF devices exhibited no particular $\Delta I(t)$ fluctuations. (b) When complementary nucleotides were present, however, sequences of two-level fluctuations were observed. (c) Non-complementary nucleotides failed to produce similar signals. (d) High magnification of data during two closing transitions of KF. (e) Single-molecule probability distributions for the timing of transitions.

Recordings of continuous catalytic processing by KF for long durations enabled reliable statistical analysis. Fig. 4d magnifies the record of Fig. 4b to show our definitions of the timing durations τ_{open} and τ_{closed} and the excursion magnitude *H*. After enumerating all of the transitions in a data record, probability distributions were built for each parameter (Fig. 4e). While the mean values τ_{open} and τ_{closed} were distinct for each type of nucleotide, the distributions of many events were broad and overlapping. τ_{open} and τ_{closed} followed simple exponential distributions with single time constants. Combinations of 16 different nucleotides and templates were measured and analyzed in the similar manner, as reported previously.[6] Comparative analysis noted differences in the incorporation rates and statistical variances for different pairs. For example, the time required to form a dA-dT base pair proved to be twice as long as for forming a dC-dG base pair, on average.

Each single excursion could also be characterized by its amplitude *H*. Histograms of *H* for each complementary base pairing exhibited a major peak for the baseline current and a minor ΔI excursion peak corresponding to KF's closed conformation. On average, a dTTP incorporation produced an excursion $\langle H \rangle$ = -6 nA, whereas a dGTP incorporation produced an excursion $\langle H \rangle$ = -2 nA, suggesting different degrees of KF closure.

5. PROTEIN KINASE A

cAMP-dependent protein kinase A (PKA) plays critical roles regulating other proteins' and enzymes' activity for cell signaling, transcription, and metabolism.[23-25] In addition to a wide range of substrate binding in its versatile active sites, PKA binds two cofactors, Mg^{2+} and adenosine-5'-triphosphate (ATP). In the presence of these cofactors, PKA catalyzes phosphorylation of target proteins by transferring the gamma phosphate from ATP.[25-27]

For electronic experiments, we synthesized the catalytic subunit of PKA with a cysteine mutation (T32C) and then attached it to SWNT devices. As in the previous cases, this particular mutation was designed to minimize interference of the SWNT attachment with PKA's binding sites or native activity. Electronic recordings were acquired with the device submerged in a standard buffer (100 mM MOPs, 9 mM $MgCl_2$, 100 μM TCEP, pH 7.2). Devices were measured in the presence of ATP (2 mM), the synthetic peptide substrate Kemptide (100 μM), or mixtures of ATP and Kemptide.

Figs. 5a and 5b show typical recordings of the current fluctuations $\Delta I(t)$ from single-molecule PKA devices. Individual binding events were visible when the devices were measured in the presence of either ATP (Fig. 5a) or Kemptide (Fig. 5b). In both cases, NMR measurements have shown that PKA only partially closes to an intermediate configuration.[28, 29]

Figs. 5c and 5d depict the arithmetic mean durations $\langle t_{Bound} \rangle$ and $\langle t_{Unbound} \rangle$, calculated in 1-s increments, for ATP and Kemptide, respectively. The mean value $\langle t \rangle$ illustrates many consecutive seconds memory in which periods with longer or shorter events to persist through many thousands of ATP or Kemptide binding/unbinding cycles. This variability and memory effect indicate a strong correlation between PKA conformational motions and ATP or Kemptide binding/unbinding, suggesting potential PKA regulation mechanisms.

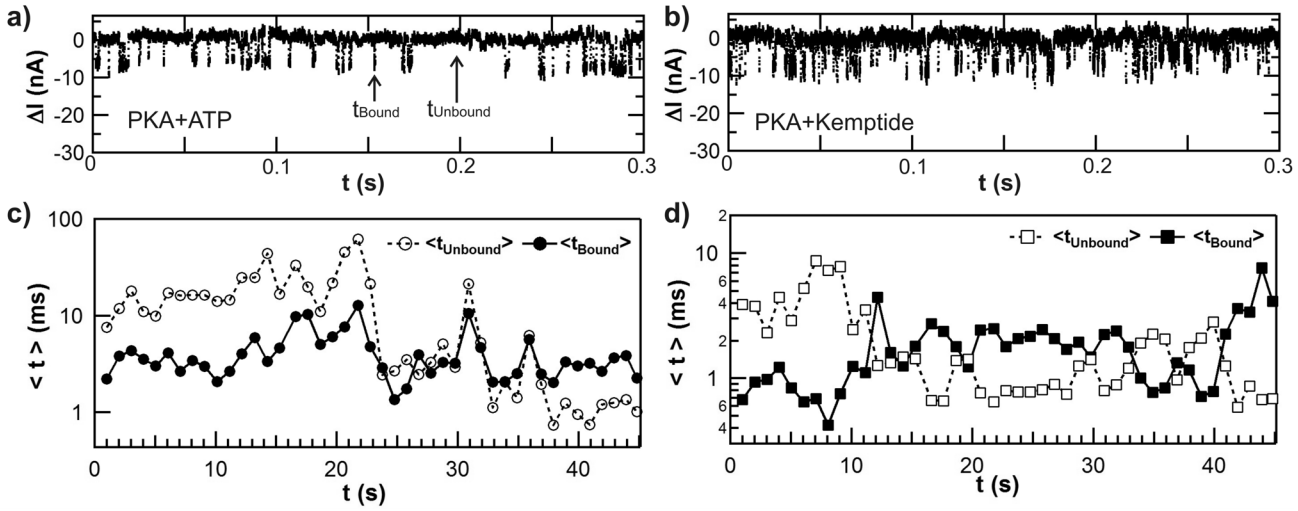

Figure 5. Electronic recordings of PKA activity during binding to (a) ATP or (b) Kemptide. From one second to another, the mean bound and unbound times for (c) ATP and (d) Kemptide vary widely over more than one order of magnitude.

When PKA has bound to both ATP and Kemptide, it can transition from its intermediate conformation to a fully-closed conformation. In this ternary complex, PKA becomes catalytically active and phosphorylation of the substrate occurs. In the presence of both ATP and Kemptide, the electronic PKA devices exhibited three-level switching that is depicted in Fig. 6a. In addition to the previous stable current levels corresponding to the open and intermediate conformations, a third current level is now observed due to formation of the ternary complex. The detailed record directly captured the two-step binding sequence in $\Delta I(t)$ that takes PKA from its initial, open configuration, through the intermediate configuration and to the fully-closed state.

Analysis of such sequencing allowed us to closely inspect PKA's catalytic cycle. Fig. 6b presents two example reaction trajectories. In one case, the recording suggests a simple trajectory from open, to intermediate, to closed, and then open again. While this type of trajectory was the most common observed, we also observed examples in which PKA re-closed multiple times before finally re-opening. Fig. 6b shows an extreme example in which 9 closures occurred without PKA fully re-opening. Because product release is associated with successful phosphorylation, we have interpreted the lack of opening as repeated, unsuccessful catalytic cycles in which multiple closures represent repeated attempts at phosphorylation. We suspect that PKA allows a mechanical reorientation of the substrate during each partial opening. Fig. 6c categorizes over 10,000 catalytic turnovers according to the number of closures observed in each. Most turnover events (77%) follow the simplest possible trajectory with a mean turnover rate of 155 s^{-1}, but at least 10% of events require 3 or more repeated closures with a much slower turnover rate averaging 37 s^{-1}.

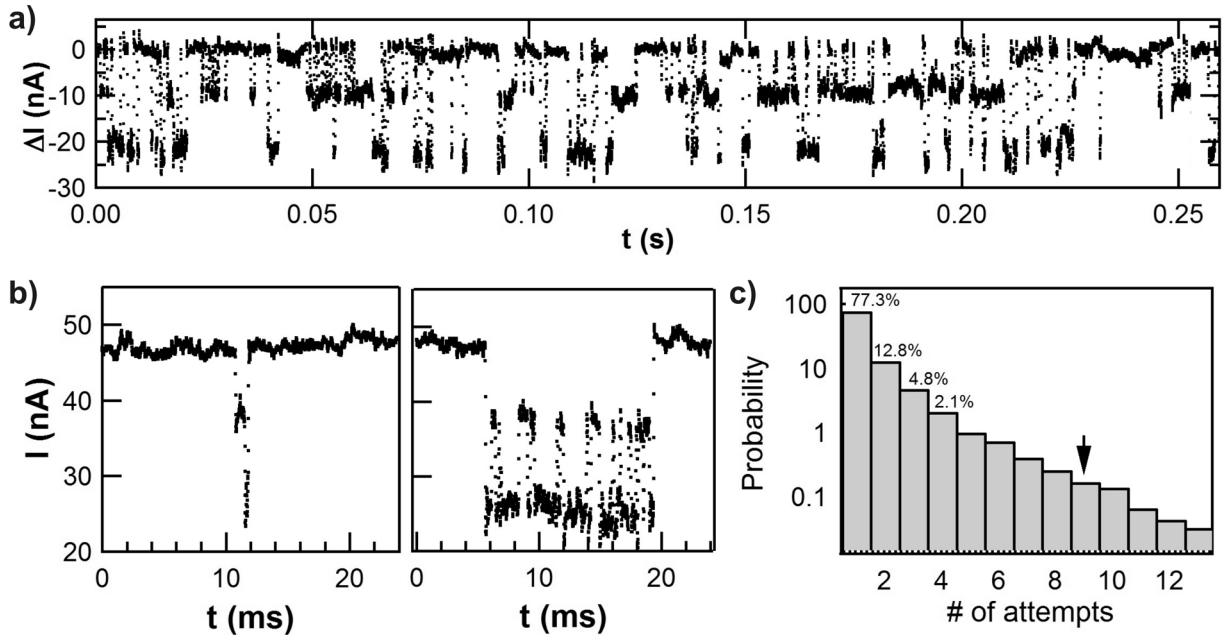

Figure 6. Electronic recordings of PKA activity in the presence of both ATP and Kemptide. (a) Three different current levels are observed corresponding to the open, intermediate, and fully-closed conformations of PKA. (b) Typical transitions consist of an excursion to the intermediate state, followed by complete closure and a return to the open conformation. However, the long-duration record also has examples of multiple closures, as shown here. (c) Probability distribution of the catalytic cycle suggests that phosphorylation proceeds successfully in 77% of the events.

6. CONCLUSION

This article has summarized recent progress fabricating practical and useful electronic devices at the molecular scale. The fabrication techniques did not require precise, high resolution lithography nor other nonstandard techniques, but the results were nonetheless highly impactful. By attaching single copies of enzymes to nanoelectronic circuits, we have demonstrated a method of single molecule characterization that allows researchers to interrogate complex, biochemical processes with unprecedented resolution. Initial experiments with these devices revealed new information about three different enzymes, two of which had already been extensively studied by single molecule FRET. The nanoelectronic device platform provides microsecond temporal resolution and allows for unlimited-duration monitoring of a single molecule's reaction trajectory, both of which are substantial improvements over more standard single-molecule

techniques like FRET. Furthermore, the bioelectronic technique is uniquely able to generate detailed recordings of single molecule activity in cases where fluorescent labeling is not possible or undesirable. The ability to monitor protein binding or enzymatic activity in the presence of multiple cofactors, or under the influence of a particular mutation, promises to grow into a powerful tool for biological sciences and pharmaceutical development.

Acknowledgements. The work described here resulted from a fruitful, long-term collaboration between research groups in physics and chemistry, and would not have been possible without the contributions of many talented students and postdocs. The work has been supported from its inception by the National Science Foundation (DMR-0801271, DMR-1104629, and ECCS-1231910) and the National Cancer Institute of the NIH (R01 CA133592-01).

REFERENCES

[1] R. Roy, S. Hohng, and T. Ha, "A practical guide to single-molecule FRET," Nature Methods, 5(6), 507-516 (2008).
[2] Y. Choi, I. S. Moody, P. C. Sims *et al.*, "Single-Molecule Lysozyme Dynamics Monitored by an Electronic Circuit," Science, 335, 319-324 (2012).
[3] Y. Choi, T. J. Olsen, P. C. Sims *et al.*, "Dissecting Single-Molecule Signal Transduction in Carbon Nanotube Circuits with Protein Engineering," Nano Letters, 13, 625-631 (2013).
[4] Y. Choi, I. S. Moody, P. C. Sims *et al.*, "Single Molecule Dynamics of Lysozyme Processing Distinguishes Linear and Cross-linked Peptidoglycan Substrates," Journal of the American Chemical Society, 134, 2032-5 (2012).
[5] P. C. Sims, I. S. Moody, Y. Choi *et al.*, "Electronic Measurements of Single-Molecule Processing by protein kinase A," Journal of the American Chemical Society, 135(21), 7861–7868 (2013).
[6] T. J. Olsen, Y. Choi, P. C. Sims *et al.*, "Electronic Measurements of Single-Molecule Processing by DNA polymerase I (Klenow fragment)," Journal of the American Chemical Society, 135(21), 7855–7860 (2013).
[7] G. Gruner, "Carbon nanotube transistors for biosensing applications," Analytical and Bioanalytical Chemistry, 384(2), 322-335 (2006).
[8] A. Star, J. C. P. Gabriel, K. Bradley *et al.*, "Electronic detection of specific protein binding using nanotube FET devices," Nano Letters, 3(4), 459-463 (2003).
[9] A. Star, V. Joshi, T. R. Han *et al.*, "Electronic detection of the enzymatic degradation of starch," Organic Letters, 6(13), 2089-2092 (2004).
[10] K. Besteman, J. O. Lee, F. G. M. Wiertz *et al.*, "Enzyme-coated carbon nanotubes as single-molecule biosensors," Nano Letters, 3(6), 727-730 (2003).
[11] H.-M. So, K. Won, Y. H. Kim *et al.*, "Single-Walled Carbon Nanotube Biosensors Using Aptamers as Molecular Recognition Elements," Journal of the American Chemical Society, 127(34), 11906-11907 (2005).
[12] P. G. Collins, [Defects and disorder in carbon nanotubes] Oxford Univ. Press, Oxford(2010).
[13] G. T. Hermanson, [Bioconjugate Techniques] Academic Press, Inc., Chicago(2008).
[14] R. J. Chen, Y. G. Zhan, D. W. Wang *et al.*, "Noncovalent sidewall functionalization of single-walled carbon nanotubes for protein immobilization," Journal of the American Chemical Society, 123(16), 3838-3839 (2001).
[15] C. Li, M. Curreli, H. Lin *et al.*, "Complementary Detection of Prostate-Specific Antigen Using In2O3 Nanowires and Carbon Nanotubes," Journal of the American Chemical Society, 127(36), 12484-12485 (2005).
[16] R. Kuroki, L. H. Weaver, and B. W. Matthews, "Structure-based design of a lysozyme with altered catalytic activity," Nature Structural Biology, 2(11), 1007-1011 (1995).
[17] R. Kuroki, L. H. Weaver, and B. W. Matthews, "A covalent enzyme-substrate intermediate with saccharide distortion in a mutant T4 lysozyme," Science, 262(5142), 2030-2033 (1993).
[18] Y. Chen, D. H. Hu, E. R. Vorpagel *et al.*, "Probing single-molecule T4 lysozyme conformational dynamics by intramolecular fluorescence energy transfer," Journal of Physical Chemistry B, 107(31), 7947-7956 (2003).
[19] S. N. Xie, "Single-molecule approach to enzymology," Single Molecules, 2(4), 229-236 (2001).
[20] D. Hu, and H. P. Lu, "Placing single-molecule T4 lysozyme enzymes on a bacterial cell surface: Toward probing single-molecule enzymatic reaction in living cells," Biophysical Journal, 87(1), 656-661 (2004).
[21] H. P. Lu, "Single-molecule spectroscopy studies of conformational change dynamics in enzymatic reactions," Current Pharmaceutical Biotechnology, 5(3), 261-269 (2004).
[22] Y. Wang, and H. P. Lu, "Bunching effect in single-molecule T4 lysozyme nonequilibrium conformational dynamics under enzymatic reactions," Journal of Physical Chemistry B, 114(19), 6669-6674 (2010).
[23] T. A. Steitz, "DNA polymerases: Structural diversity and common mechanisms," Journal of Biological Chemistry, 274(25), 17395-17398 (1999).

[24] E. Delagoutte, "DNA polymerases: Mechanistic insight from biochemical and biophysical studies," Frontiers in Bioscience-Landmark, 17, 509-544 (2012).
[25] J. A. Adams, "Kinetic and catalytic mechanisms of protein kinases," Chemical Reviews, 101(8), 2271-2290 (2001).
[26] B. E. Kemp, D. J. Graves, E. Benjamini *et al.*, "Role of multiple basic residues in determining the substrate specificity of cyclic AMP-dependent protein kinase," Journal of Biological Chemistry, 252(14), 4888-94 (1977).
[27] J. A. Adams, and S. S. Taylor, "Energetic limits of phosphotransfer in the catalytic subunit of cAMP-dependent protein kinase as measured by viscosity experiments," Biochemistry, 31(36), 8516-22 (1992).